Post-print of Catalysis Science & Technology, Volume 7, Issue 13, 24 may 2017, Pages 2886-2896

Low temperature total oxidation of toluene by bimetallic Au-Ir catalysts

Laura Torrente-Murciano[a], Benjamín Solsona[b], Saïd Agouram[c], Rut Sanchis[b], José Manuel López[d], Tomás García[d] and Rodolfo Zanella[e]

[a] *Department of Chemical Engineering and Biotechnology, University of Cambridge, Philippa Fawcett Drive, CB3 0AS, Cambridge, UK*
[b] *Department d'Emginyeria Quimica, Universitat de Valencia, 46100 Burjassot, Valencia, Spain*
[c] *Department of Applied Physics and Electromagnetism, University of Valencia, Burjassot 46100, Spain*
[d] *Instituto de Carboquímica (ICB-CSIC), 50018 Zaragoza, Spain*
[e] *Centro de Ciencias Aplicadas y Desarrollo Technológico (CCADET), Universidad Nacional Autónoma de México (UNAM), Ciudad de Mexico, Mexico*

Abstract

Bimetallic gold-iridium catalysts present a synergetic activity effect for the total oxidation of volatile organic compounds (e.g. toluene) respect to their monometallic counterparts, leading to catalytic activity at lower temperature. The enhancement of activity is facilitated by the intimate contact of the iridium and gold species, which modifies the electronic environment of the active sites, assisting in the oxygen activation at lower temperature. In addition, the bimetallic system show a considerably higher metal-support interaction capable of diminishing the detrimental loss of activity associated to metal sintering at high reaction temperatures, in contrast to the monometallic cases whose activity is greatly lost. This paper contributes to the understanding of the key factors behind high activity and high stability of catalysts to enable the low temperature activity of VOC compounds in air pollution remediation applications.

Keywords: VOCs; Total oxidation; gold; iridium: propane; toluene, bimetallic.

1. Introduction

Volatile organic compounds (VOCs) emissions are one of the main sources of global air pollution, believed to influence the climate through their involvement in the production of organic aerosols, ozone and smog via photochemical reactions [1]. The largest source of natural VOC emissions is from vegetation, and oceans in minor extent. On the other hand, anthropogenic emissions include a variety of sources from chemical, pharmaceutical, biomass and power plants to cleaning products, domestic cooking or office supplies [2]. VOC concentrations are predominantly higher close to their source area, primarily in heavily populated and industrialised regions. Due to the health issues associated to most of the VOCs compounds, their emissions are currently regulated including their elimination via adsorption, filtration, and thermal and catalytic oxidation [3]. Out of them, the total catalytic oxidation of VOCs is highly attractive for both outdoor and indoor applications due to their complete combustion into harmless and less-harmful products (H_2O and CO_2).

Two main types of catalysts have been developed during the last decades for the total oxidation of VOCs, including transition metal oxides and supported noble metal catalysts. While transition metal oxides such as ceria present advantages in terms of availability and cost [4, 5], higher activities are achieved with palladium and platinum-based systems [6]. The current challenge lays on the development of low temperature systems active for a wide range of VOCs compounds with high stabilities. Within this context, gold-based catalysts are believed to be advantageous over other noble metals for reactions at low temperature because the bonding strength of adsorption of gold defective sites is moderate and still weaker than that of palladium and platinum [7]. The activity of gold-based catalysts is directly related to its interaction with the support, with reducible oxides showing up to one order of magnitude higher activities than inert supports [8-10]. Additionally, a strong synergetic effect has been

observed between gold and TiO_2 [2, 11]. However, gold particles typically nucleate at the O-defect sites of reducible oxides such as TiO_2, which after heating, inevitable lead to their sintering as the gold metal cohesive energy is generally larger than the Au-oxide bonding energy [12]. This metal-support interaction is a key parameter in the design of stable catalysts, an aspect usually underestimated in academic research. Indeed, a recent review of the use of supported gold catalysts for the total oxidation of VOC by Scire and Liotta [2] concluded that not enough attention has been devoted to the stability of Au-based catalysts under reaction conditions, which appears to be a major drawback for any commercial application in this field.

The addition of a second metal to gold can affect the stability of the catalyst and enhance its resistance versus sintering as recently demonstrated theoretically in gold-iridium systems using DFT calculations [13]. Moreover, it is known that the addition of a second metal forming both alloys and core-shell particles can also have an electronic effect on the gold active sites enhancing their activity and selectivity in a wide range of reactions [14, 15]. The interaction between both metals depends on their nature and the conditions which they are exposed.

In this paper, we present the effects of adding iridium to gold catalysts supported on TiO_2 by a sequential deposition-precipitation method previously developed by Zanella's group [16]. We demonstrate that the total oxidation of toluene takes place at considerably lower temperatures on the Au-Ir/TiO_2 catalyst compared to it gold-only or iridium-only counterparts. This synergetic effect is based on an electronic effect of gold by the presence of iridium which not only modifies its activity but also its reducibility and stability.

2. Experimental

Synthesis of the catalysts

Gold and iridium were supported on commercial titania (Evonik P25) by a deposition-precipitation with urea (DPU) previously reported by Zanella's group [17]. The monometallic Au/TiO_2 and Ir/TiO_2 catalysts were prepared in the absence of light using $HAuCl_4$ and $IrCl_4$ as metal precursors respectively. A 50 mL aqueous solution of the corresponding metal concentration and urea (0.42 M) was prepared to which, the TiO_2 support was added before increasing the temperature to 80°C and stirred for 16 hours. After the deposition-precipitation of the metals, the samples were washed and dried under vacuum at 80°C.

The bimetallic $Au\text{-}Ir/TiO_2$ catalyst was prepared by sequential deposition-precipitation with urea. In this case, the Ir/TiO_2 catalyst prepared as described above, was calcined in air at 500 °C for 2h prior depositing gold using the same method.

Catalyst characterisation

Morphological and structural characterization of the samples was performed by transmission electron microscopy (TEM) and high resolution TEM (HRTEM) by using a FEI Field Emission Gun (FEG) *TECNAI G^2 F20 S-TWIN* microscope operated at 200 kV. The mean size of the metal nanoparticles was determined from HRTEM images using the following equation:

$$Mean\ size = \frac{\sum(d_i \cdot n_i)}{\sum n_i}$$

where d_i is the particle diameter and n_i is the number of particles with a diameter d_i. Around 100 particles were used to estimate the mean size although the exact number depends on the catalyst. Energy Dispersive X-rays Spectroscopy (EDS) in TEM nanoprobe mode was achieved to prove the purity of the synthetized Au and Ir nanoparticles and to determine the composition of Au-Ir crystals. The samples were prepared by sonication in absolute ethanol

for few minutes and a drop of the resulting suspension were deposited onto a holey-carbon film supported on a copper grid, which was subsequently dried.

Powder X-Ray diffraction (XRD) was used to identify the crystalline phases present in the samples. A Bruker D8 Advance diffractometer with monochromatic Cu Kα source operated at 40 kV and 40 mA was used. The experimental patterns were calibrated against a silicon standard and the crystalline phases were identified by matching the experimental patterns to the JCPDS powder diffraction file database.

X-ray photoelectron spectroscopy (XPS) measurements were made on a Kratos Axis ultra DLD photoelectron spectrometer using a non-monochromatized Mg Kα X-ray source (hν = 1253.6 eV). An analyser pass energy of 50 eV was used for survey scans and 20 eV for detailed scans. Binding energies were referenced to the C1s peak from adventitious carbonaceous contamination, assumed to have a binding energy of 284.8 eV. XPS data were analysed using CasaXPS software. All the peaks of the corrected spectra were fitted with a Gaussian–Lorentzian shape function to peak fit the data. Iterations were performed using the Marquardt method. Relative standard deviations were always lower than 1.5%.

Temperature programmed reductions (TPR) analyses were carried out in a Micromeritics Autochem 2920 rig equipped with a TCD detector under a 50 mL min^{-1} 5% H_2/Ar flow at temperatures between room temperature and 450°C with a heating rate of 10°C min^{-1}. CO pulse chemisorption analyses were carried out in the same equipment under cryogenic conditions after treatment the catalyst at 400°C under a flow of 20 mL min^{-1} of helium. After complete CO chemisorption, temperature programme desorption analyses were carried out by increasing the temperature up to 400°C under a flow of 50 mL min^{-1} of helium.

Raman spectra were obtained using a Horiba Jobin Yvon HR800 UV dispersive laser Raman microscope. The excitation source used was an argon ion laser (532 nm) operated at a power

of 26 mW and at room temperature. The laser was focused on powdered samples placed on a microscope slide to produce a spot size ca. 3 ∝m in diameter. A backscattering geometry with an angle of 180^{o} between illuminating and collected radiation was used for recording data. The acquisition time was 60 s for each spectrum with a spectral resolution of 1 cm^{-1}.

Catalytic studies

The total oxidation of toluene was studied using 100 mg of catalyst loaded into a quartz micro reactor (inner diameter 7 mm) to give a GHSV of 27000 h^{-1}. The feed gas contained 833 ppm of toluene diluted in synthetic air (toluene/O_2/He with a molar ratio of 0.0833/20/80). The temperature ramp used was 5ºC/min. Once the desired reaction temperature was achieved and after a stabilization period of 45 min two analyses were carried out and the results averaged. Several cycles have been conducted on representative catalysts in order to check the stability, the data plotted corresponding to heating cycles. Once the first cycle was finished (after reaching 100% conversion), the catalyst was cooled down just switching off the oven in a helium stream (20 ml min-1). The catalyst was kept overnight at room temperature also in flowing helium. The second cycle was started the subsequent day and the same procedure was applied. The third run was conducted in a similar way. The outlet gas was analysed by online gas chromatography, using a Hewlett-Packard apparatus equipped with both TCD and FID detectors and two columns: (i) Carbosieve-S and (iii) Porapak Q.

3. Results

Catalytic activity for toluene total oxidation

A series of gold and iridium catalysts supported on TiO_2 was prepared by sequential deposition-precipitation with urea. The catalysts were tested for the total oxidation of toluene, a model aromatic compound classified as one of the most challenging VOCs molecules for total oxidation [18]. The bimetallic Au-Ir/TiO_2 catalyst shows activity towards the total oxidation of toluene at temperatures as low as 100°C, reaching full conversion under the studied conditions at 275°C (Figure 1). On contrast the monometallic catalysts present activity at considerably higher temperatures. The monometallic Au/TiO_2 catalysts shows activity at temperatures above 200°C and the Ir/TiO_2 catalyst is only active at temperatures above 225°C, with a lower conversion than its gold-only counterpart catalyst at a given temperature. Mass balances were closed at 100 ± 4 wt. % in all cases and only total oxidation products were detected.

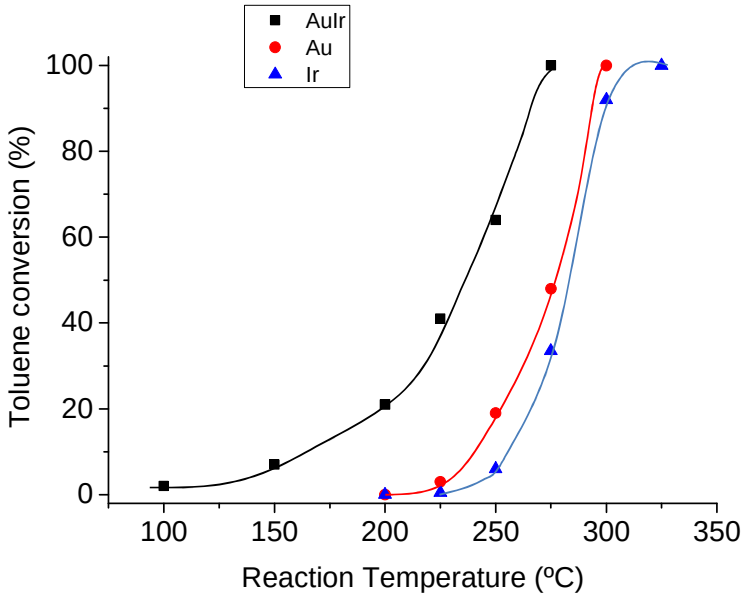

Figure 1: Catalytic conversion of toluene respect to temperature using ● Au/TiO_2, ▲ Ir/TiO_2 and ■ Au-Ir/TiO_2 catalysts (first heating run).

Figure 1 shows clear synergetic effect on the bimetallic catalyst activity respect to the mono-metallic ones where Ir promotes the performance of Au active sites by facilitating the oxygen

mobility at the gold-support interlayer. Indeed, an increase in the reaction rate of more than one order of magnitude is obtained in the bimetallic catalyst compared to the pure Au or Ir catalysts (Table S1). It is important to highlight that this synergetic effect is not observed when a physical mixture of Au/TiO_2 and Ir/TiO_2 catalysts is used. In this case, a higher activity is observed at a given temperature respect to the mono-metallic counterparts due to the increase of active sites, however, similar temperature of activation are observed than in the mono-metallic cases (Figure S1).

A more exhaustive catalytic study dealing with the robustness of these samples was conducted on the most active monometallic (Au/TiO_2) and on the bimetallic Au-Ir catalyst. Firstly, the stability of the $Au\text{-}Ir/TiO_2$ catalysts under reaction conditions was investigated. Three consecutive catalytic cycles were run as shown in Figure 2a. A very small decrease in catalytic activity of $Au\text{-}Ir/TiO_2$ was observed after the first cycle at temperatures below 200ºC, and over that temperature a stable activity is observed in consecutive runs suggesting that a steady state is reached. In the Au/TiO_2 catalyst a stable activity was also observed regardless of the cycle considered. In all cases, the catalysts remain stable in further consecutive runs, indicating the high stability of mono- and bi-metallic catalysts at moderate temperatures (up to 300 °C).

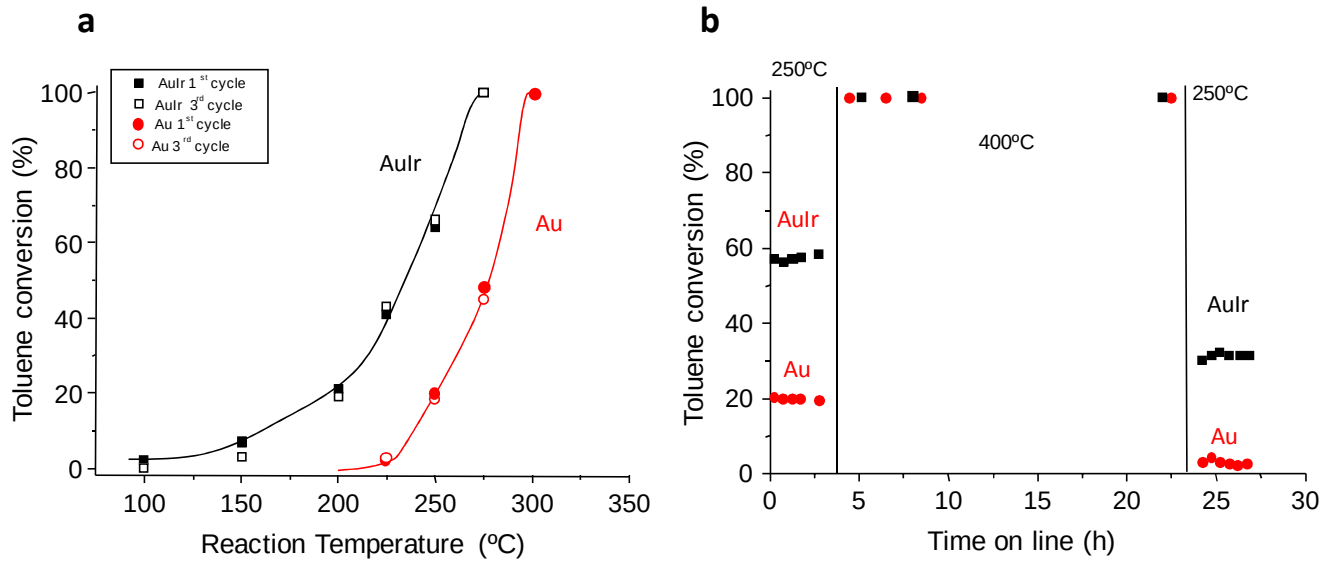

Figure 2: Catalytic stability in toluene oxidation of monometallic Au/TiO_2 and bimetallic Au-Ir/ TiO_2 catalysts. a) consecutive catalytic cycles, b) variation of the toluene conversion with the time (3 h at 250ºC followed by 20 h at 400ºC and 3h at 250ºC). Reaction conditions detailed in text.

In order to study the stability of the catalysts at higher temperatures, another more demanding test was designed. Au/TiO_2 and Au-Ir/TiO_2 catalysts were maintained under reaction conditions during prolonged times at high temperature (400ºC). As it can be observed in Figure 2b, Au-Ir/TiO_2 catalyst presents a constant toluene conversion at 250°C during 3 hours of operation. A similar effect is observed with the counterpart monometallic Au/TiO_2 catalyst. After a certain period of time, the reaction temperature was increased to 400°C for 20 hours, where both catalysts show a constant 100% conversion. Finally, the reaction temperature was decreased back to 250°C and maintained for few hours. In both cases, with the bimetallic and monometallic catalysts, a decrease of activity was observed with respect to the activity of the fresh catalysts at 250°C, however, the decrease in activity is considerably lower in the case of the Au-Ir/TiO_2 catalysts (decrease of 45% of the initial activity) respect to the monometallic Au/TiO_2 one (decrease of 85%), which is almost completely deactivated.

Therefore, according to the catalytic study conducted, we can state that a clear synergetic effect is observed between Au and Ir as the bimetallic catalyst is considerably more active than both monometallic catalysts. Moreover, all mono- and bi-metallic catalysts are highly stable if working at temperatures below 300ºC but if they are treated in reaction conditions at 400ºC the catalytic performance deteriorates. Interestingly, the deactivation of bimetallic Au-Ir/TiO_2 catalyst is remarkably lower than that of Au/TiO_2 catalyst.

Characterization results

The bulk and surface atomic compositions of the different mono- and bi-metallic systems determined by EDS and XPS are shown in Table 1. The measured bulk metal loadings are slightly higher that the nominal amount but the Au/Ir atomic ratio is close to 1. As expected,

enrichment in the metal surface composition is observed for both gold and iridium species, being more relevant for gold nanoparticles. Additionally, partial covering of iridium nanoparticles after gold deposition-precipitation is not apparent since both Ir/TiO_2 and $Au-Ir/TiO_2$ show comparable surface and bulk compositions after gold incorporation.

Table 1: Surface and bulk atomic composition of the fresh monometallic and bimetallic Au and Ir catalysts

Catalyst	Bulk (EDS)		Surface (XPS)	
	%at Ir	%at Au	%at Ir	%at Au
Au/TiO_2		1.2		2.4
Ir/TiO_2	1.0		1.5	
$Au-Ir/TiO_2$	1.1	1.2	1.5	2.3

The synergetic effect observed by the Au-Ir system was investigated by detailed physical and chemical characterisation of both the mono- and bi-metallic catalysts. Firstly, the metal particle size of the different catalysts was investigated by microscopy. Figure 3 shows representative TEM micrographs of the Au, Ir and Au-Ir samples supported on TiO_2. In both fresh and catalysts used in reaction, metal nanoparticles are homogeneously distributed on the TiO_2 matrix. It is worth pointing out that Ir nanoparticles are hardly visible but can be detected by a microscopy analysis. For gold-based catalysts the density was ranging from 6200 to 7500 NPs/$\backsim m^2$. **¡Error! No se encuentra el origen de la referencia.** presents particle size histograms of fresh monometallic Au and bimetallic Au-Ir catalysts. As we can observe in the histograms, fresh catalysts show a quite narrow distribution with nanoparticles ranging between 1 and 3 nm with the absence of agglomeration. It is of interest to note that the histogram of Ir nanoparticles has not been made because the grain size measurement is not very accurate, but an average size around 1.5 nm ± 0.5 nm is detected. All the nanoparticles are well distributed on TiO_2 matrix. These observations are in agreement with those calculated using CO chemisorption, with average metal particles of 1.6, 1.2 and 1.8 nm corresponding to the Au/TiO_2, Ir/TiO_2 and $Au-Ir/TiO_2$ catalysts, respectively. A

stoichiometric factor of 1 was used for the Au-CO chemisorption experiments while a value of 2 was used in the Ir-CO cases [19]. Semi-spherical particles are assumed in all cases with its associated experimental error [20]. These values of metal particles are also in agreement with the lack of apparent diffraction peaks either corresponding to Au- or Ir-containing phases by XRD, likely to be below the detection limit (< 3 nm) (Figure S2). Although metal particle size is known to have a strong effect on their reactivity [7], the small differences of particle sizes is not believed to be responsible for the difference of activities between the monometallic and bimetallic Au-Ir/TiO_2 catalysts.

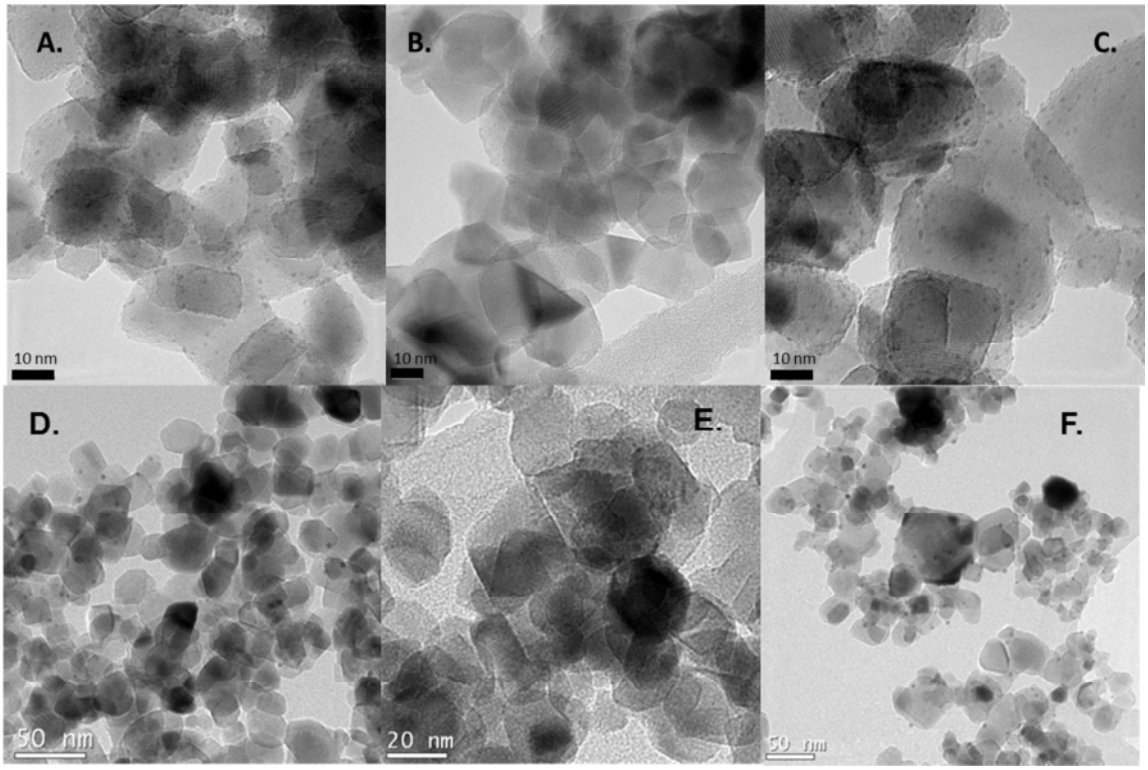

Figure 3: TEM bright micrographs of A. Au/TiO_2, B. Ir/TiO_2 and C. Au-Ir/TiO_2 fresh catalysts and D. Au/TiO_2, E. Ir/TiO_2 and F. Au-Ir/TiO_2 samples used in toluene oxidation after 3 cycles.

To further understand the effect of metal agglomeration in the loss of activity, TEM studies of the catalysts after i) 3 cycles up to 300ºC and ii) after 20 hours reaction at 400°C were undertaken. An increase in particle size was observed in both, the mono- and bi-metallic gold-based catalysts, although the sintering degree is rather different in both cases, see Figure

4. Gold particle size distribution of the monometallic Au/TiO_2 catalyst shifts from 1-3 nm to 2-7 nm after the three consecutive cycles whereas it dramatically increases up to 5-20 nm after the prolonged reaction at 400°C. In the case of the bimetallic $Au\text{-}Ir/TiO_2$ an agglomeration of gold particles is observed from 1-4 nm to 2-8 nm after three consecutive cycles, whereas after the prolonged test at 400ºC the gold size increases up to 3-10 nm. Thus, the presence of iridium mitigates the aggregation of particles of the bimetallic catalyst if compared to the Ir-free Au/TiO_2 catalyst. Finally, Ir/TiO_2 catalyst used for 3 cycles showed an increase of about 0.5 nm compared to the fresh sample; thus the average size was about 2 ± 0.5 and the nanoparticles are also well distributed on the support.

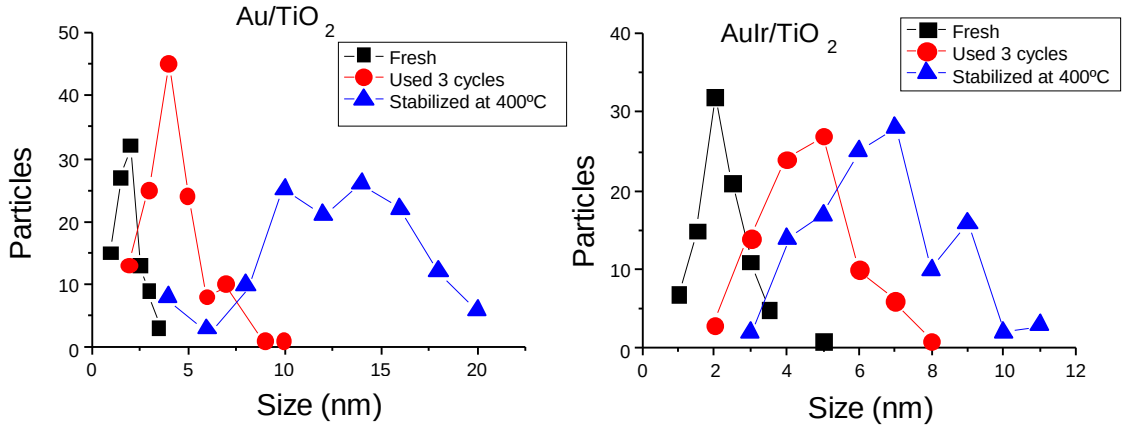

Figure 4: Particle size distribution histograms determined by TEM of Au/TiO_2 and $Au\text{-}Ir/TiO_2$ catalysts.

HRTEM characterization was conducted in order to obtain clear information about the crystalline structure of the metal nanoparticles, allowing the accurate determination of their lattice parameter. It is worth mentioning that as the density of the nanoparticles is relatively low, the determination of crystalline structure and lattice parameter from Selected Area Electron diffraction (SAED) can have a certain error. Figure 5 shows a representative HRTEM image of gold nanoparticles on the TiO_2 matrix where it can be observed that the

nanoparticles are single crystals, as clearly indicated by the atomic lattice fringes. The analysis of HRTEM image of TiO_2 and its digital diffraction pattern (FFT) also confirms its crystalline structure. Lattice fringes and diffraction spots in FFT image are clearly identified and lattice planes of the anatase crystal structure with an interplanar distance of 3.53 and 2.41 Å corresponding to the (101) and (103) planes respectively, are observed (Ref. JCPDS: 021-1272). The difference in lattice parameters of Au [4.07 Å; JCPDS: 04-0784] and Ir [3.83 Å; JCPDS. 01-1212] could help us to establish the potential bimetallic character of the nanoparticles by analysing the interplanar distances observed HRTEM images. In fact, direct measurement of spacing between the crystal fringes of Au-Ir bimetallic nanoparticles is about 2.375-2.400 Å corresponding to the lattice spacing of (111) planes of the cubic phase structure of gold [JCPDS: 04-0784] with space group Fm3m. The measured a-lattice parameters were found to be between 4.114 - 4.157 ± 0.015 Å, which is higher than that of pure Au nanoparticles. It is of interest to notice that no diffraction spots were observed that could be indexed to the cubic structure of iridium crystals. Nowadays, the incorporation of Ir atoms in Au lattice or/and vis-versa is a controversial subject. A. Aguirre et al. [21] observed that Au-Ir/CeO_2 catalyst shows a lattice spacing of 0.231 nm, which was between that of the Ir (111) plane (0.219 nm) and the Au (111) plane (0.235 nm), indicating the formation of the surface Au–Ir alloy; whilst other works have concluded that gold and iridium are practically immiscible in the bulk [22], being the formation of an alloy unfavourable. In our case, we observe a shift to higher values in the lattice parameter instead of an intermediate value, suggesting that Au-Ir alloy is not formed. Therefore, this difference in the lattice parameter is likely to be attributed to the intimate contact between both metals, which are strongly interacting with the titania support. Localized EDS analysis in nanoprobe mode using a spot size in the order of 1-2 nm in diameter was conducted to prove the intimate contact between gold and iridium species. Thus, in fresh and used bimetallic catalyst domains containing both gold and IrO_2 are detected with a composition about 46 and 54 at % (±10 %) of Au and Ir,

respectively, whereas no isolated gold or IrO_2 crystallites are observed. Therefore, gold and the iridium phases seem to be in close contact but not forming an alloy. This intimate contact of metals, also shown by TEM, could facilitate the modification of the electronic environment of the bimetallic active sites and therefore it is likely to be responsible for the low temperature oxidation activity of the bimetallic catalyst compared to the mono-metallic ones [23].

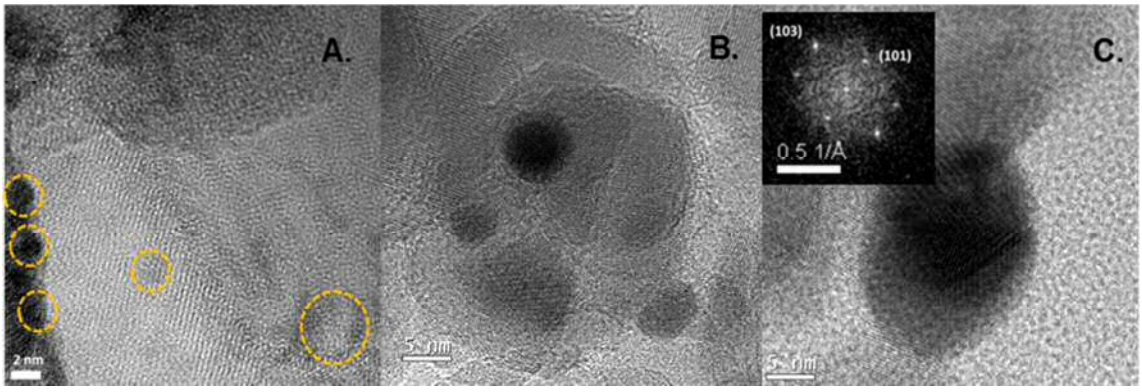

Figure 5: High resolution TEM micrograph of Au-Ir nanoparticles (highlighted in circles) supported on TiO_2. (A) fresh catalyst, (B) and (C) after used in reaction for 3 cycles.

XPS analyses of the different monometallic and bimetallic catalysts (

Figure **6**) were carried out to get further insights about the oxidation state and potential electronic modifications of the bimetallic system. Regarding the O1s and the Ti2p core-levels (not shown), relevant differences for the different samples are not found. Figure 6 shows the Au 4f core levels and the the Ir 4f core levels of fresh and used bi-metallic Au-Ir/TiO_2 catalyst. Similar XPS profiles are obtained for the monometallic Au/TiO_2 and Ir/TiO_2 respectively. It is important to note that a contribution of Ti 3s at ~ 62 eV from the support appears in the Ir 4f region. All fresh and used series of catalysts present comparable Ir4f spectra independently of being mono- or bi-metallic catalysts whilst the Au4f spectrum is different in the case of fresh catalysts compared with the used ones. The curve fitting of the Au 4f spectrum for the mono- or bi-metallic catalysts indicates two Au 4f7/2 components at

BE = 83.6-83.8 and 85.6-86.0 eV, attributed to Au^0 and Au^+ species respectively [24]. In the case of both fresh catalysts, Au/TiO_2 and $Au\text{-}Ir/TiO_2$, their relative distribution reveals a predominant contribution of metallic gold but with a 16-17 % of oxidized Au^+ on the sample surface. However, after use in reaction (3 cycles or at 400ºC) a notable difference is observed for both catalysts as no cationic gold is detected, with the only contribution of metallic gold at BE = 83.1 ± 0.1 eV.

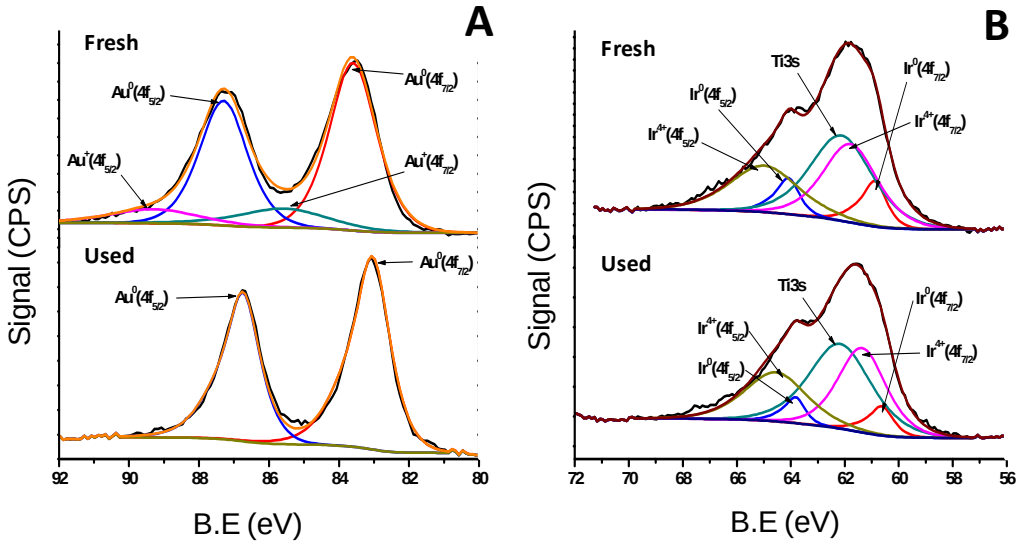

Figure 6: XPS spectra of the fresh and used after reaction Au-Ir/TiO_2 catalystFigure 6. A. Au 4f core levels and B. Ir 4f core levels.

In the case of Ir 4f core level (Figure 6B), all the Ir-containing catalysts, Ir/TiO_2 and $Au\text{-}Ir/TiO_2$, exhibit Ir 4f7/2 peaks at 60.7-60.9 eV and 61.5-61.7 eV corresponding to Ir^0 and Ir^{4+} respectively. Moreover, all fresh and used samples present comparable spectra and similar deconvolution patterns, with a predominant presence of cationic iridium. Thus the metallic oxide iridium contribution ranges between 79.7 and 85.9 %. It is important to highlight that in contrast to the results found by Zhao et al. [25], no significant shift of the binding energies

corresponding to either gold or iridium species is observed, suggesting again that the alloy formation between gold and iridium metals can be ruled out.

Table 2 also shows the Au/Ti and Ir/Ti surface ratios for the fresh and used catalysts. Used samples showed a deep reduction in the Au/Ti ratios compared with the fresh ones. After being used, the Au/Ti ratio decreased from 0.084 for the fresh samples to values c.a. 0.030 for the used ones. This feature can be related with an agglomeration process of the gold nanoparticles due to the temperature effect. In the case of Ir/Ti ratio, a different behaviour can be observed. Thus, in contrast with the bimetallic catalyst, Ir/Ti shows comparable values after thermal treatment, in agreement with TEM data. Additionally, it can be observed that the Ir/Ti value for the calcined Ir/TiO_2 catalyst hardly changes after gold deposition-precipitation, pointing out that iridium nanoparticles are not covered by gold.

Table 2: Binding energies and relative surface composition by XPS

	Au (0)		Au(δ+)		Ir(0)		Ir (4+)		Ir/Ti	Au/Ti
Catalyst	**BE (eV)**	**%at**	**BE (eV)**	**%at**	**BE (eV)**	**%at**	**BE (eV)**	**%at**		
2% Au/TiO_2 (fresh)	83.8	84.2	86.0	15.8	-	-	-	-	-	0.084
2% Au/TiO_2 (used 3 cycles)	83.1	100	-	-					-	0.038
2% Au/TiO_2 (after reaction at 400ºC)	83.1	100	-	-	-	-	-	-	-	0.031
2% Ir/TiO_2 (fresh)	-	-	-	-	60.8	14.7	61.5	85.3	0.061	-
2% Ir/TiO_2 (calcined at 500ºC)	-	-	-	-	60.8	14.7	61.5	85.3	0.051	-
2% Ir/TiO_2 (used 3 cycles)	-	-	-	-	60.9	15.3	61.7	84.7	0.049	-
2% Au-Ir/TiO_2 (fresh)	83.6	82.8	85.6	17.2	60.9	20.3	61.7	79.7	0.050	0.084
2% Au-Ir/TiO_2 (after 3 cycles)	83.2	100	-	-	60.7	14.3	61.5	85.7	0.050	0.037
2% Au-Ir/TiO_2 (after reaction at 400°C)	83.1	100	-	-	60.8	18.9	61.5	81.1	0.046	0.033

The interaction between gold and iridium in the bimetallic catalyst has also an effect on the reducibility properties of the catalyst. Figure 7 shows the temperature programmed reduction (TPR) profiles of the different fresh and catalysts used in reaction for 3 cycles. Cationic gold species present in the fresh Au/TiO_2 catalyst are reduced at ~100°C. The TPR profile of the Ir/TiO_2 catalyst is characterised by three H_2 consumption peaks at 110, 145 and 230°C [16], with complete reduction of IrO_2 achieved at 300°C. The weaker peaks at 110 and 145 ºC can be assigned to the reduction of large iridium oxide particles, whereas the peak at 230 ºC can be attributed to iridium oxide species with higher interaction with the support. Interestingly, the reduction temperatures of gold and iridium in the bimetallic $Au\text{-}Ir/TiO_2$ catalyst shift towards higher temperatures respect to their monometallic counterparts. Indeed, in this case, a single peak in the region of ~110°C shows the reduction of gold and potentially some iridium species. Additionally, the high temperature reduction peak of iridium appears at ~270°C with complete reduction of the catalyst at 450°C. This alteration of the reduction temperatures in the bimetallic system respect to the monometallic counterparts indicates again a strong interaction between gold and iridium species and/or support. A similar effect has been observed in either Au particles supported on Co_3O_4 where an electron transfer was observed from the Au to the Co_3O_4 [2] or Au nanoparticles supported on nickel-doped TiO_2 catalysts [26]. The TPR profiles of gold containing catalysts used in reaction (Au/TiO_2 and $AuIr/TiO_2$) show that the band corresponding to the reduction of cationic gold disappears, suggesting, in agreement with the XPS data, that during the toluene oxidation reaction all the oxidized gold reduces to metallic gold. Regarding to the iridium species, it can be appreciated a slight shift to lower reduction temperatures in the bimetallic $AuIr/TiO_2$ whereas hardly differences are observed in the monometallic Ir/TiO_2 catalyst. Again, the presence of gold in the bimetallic $Au\text{-}Ir/TiO_2$ sample slightly shifted the reduction temperature of the iridium species to higher temperature, suggesting that a strong interaction between gold and

iridium species and/or the support is still occurring. The hydrogen consumption was measured by comparing the thermoconductivity of the inlet and outlet gases during the TPR experiments. As expected, the hydrogen consumption during the TPR of the bi-metallic Au-Ir catalyst is higher (5.47 cm^3 H_2 g^{-1} (STP)) than that of the only Au (2.17 cm^3 H_2 g^{-1} (STP)) and only Ir (4.56 cm^3 H_2 g^{-1} (STP)) catalysts.

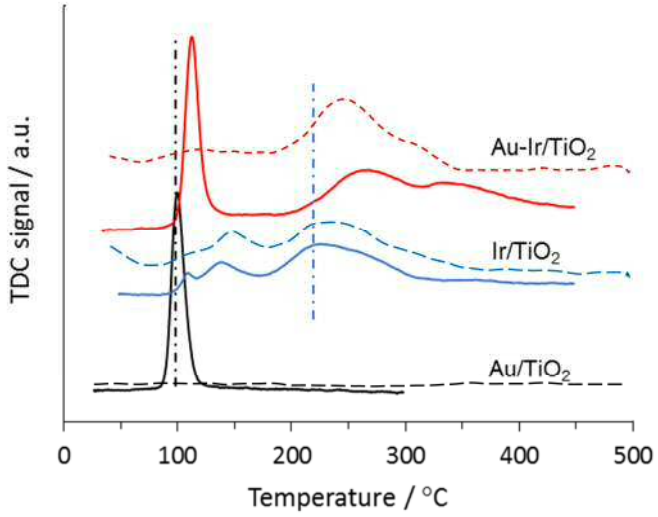

Figure 7: Temperature programmed reduction (TPR) profiles of Au/TiO_2, Ir/TiO_2 and $Au\text{-}Ir/TiO_2$ catalysts. Full lines correspond to fresh catalysts and dashed lines to catalysts used in total oxidation of toluene reaction during 3 cycles.

Metal-support interaction is also known to greatly affect the catalytic activity, especially on TiO_2 supported catalysts [15]. Consequently, the interactions between gold and iridium mono- and bi-metallic particles with the TiO_2 support were investigated by Raman spectroscopy. The Raman spectrum of TiO_2 anatase phase presents six allowed modes that appear at 144 cm^{-1} ($E_{g(1)}$), 197 cm^{-1} ($E_{g(2)}$), 399 cm-1 ($B_{1g(1)}$), 513 cm^{-1} (A_{1g}), 519 cm^{-1} ($B_{1g(2)}$) and 639 cm^{-1} ($E_{g(3)}$) respectively [27]. As shown in Figure 8, our three catalysts present the five characteristic peaks of anatase phase (A_{1g} and $B_{1g(2)}$ modes are not resolved at room temperature). The rutile phase for TiO_2 cannot be observed. The principal peak at 144 cm^{-1} characteristic of the Ti−O stretching mode in the pure TiO_2 positively shifted in the three

metallic catalysts but with different extent, being more pronounced for bimetallic catalyst (152 cm^{-1}) followed by Au/TiO_2 (150 cm^{-1}) and Ir/TiO_2 (147 cm^{-1}).

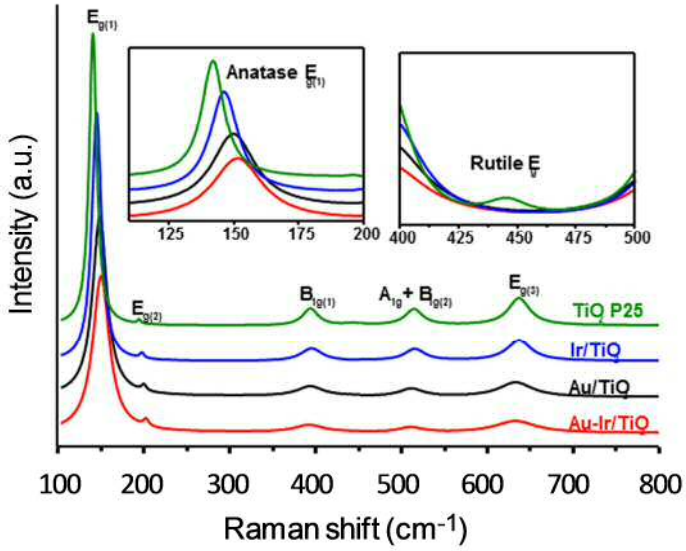

Figure 8: Raman spectra of fresh Au/TiO_2, Ir/TiO_2 and $Au\text{-}Ir/TiO_2$ catalysts. Spectrum of TiO_2 P25 is shown for comparison.

As Table 4 shows that not only the peak position has been shifted but also the broadness (FWHM) and peak intensities are different for the three catalysts. Indeed, wider and lower peak features are observed from Ir/TiO_2 → Au/TiO_2 → $Au\text{-}Ir/TiO_2$. A superimposed effect caused by both the Au and IrO_2 particles in the bi-metallic catalysts can be ruled out as this is the same order than the low temperature oxidation activity increases during the reactions. Interpretation of the variation of Raman peak shapes have been attributed to a range of factors, such as (i) a pressure effect due to the surface tension of grains, (ii) a decrease in the Ti–O bond strength, (iii) non-stoichiometry as induced by oxygen deficiency or disorder induced by some minor phases in the sample, and (iv) phonon confinement effects with the grain size variation. Since the XRD analysis showed that the difference in crystallite sizes for the three catalysts is not significant, and the same phases are detected, we can tentatively conclude that the frequency shift, the intensity decrease and the FWHM increase of the 144

cm^{-1} anatase band, are primarily associated with the presence of more oxygen defects in the TiO_2 support. In line with this, it can be observed that gold incorporation in the TiO_2 support creates more oxygen defects than iridium during the urea deposition-precipitation process, which is further increased in the bimetallic catalyst obtained by gold sequential deposition-precipitation with urea of the Ir/TiO_2 catalyst. This Raman shift to higher energies confirmed that the presence of iridium species leads to a stronger interaction between gold nanoparticles and TiO_2, promoting the formation of oxygen vacancies (crystalline defects). In line with this, it has been previously suggested that the presence of oxygen vacancies and other defects as being probable causes for stabilizing the interface of Au(111) and TiO_2 (110) [28]

Table 4: Main parameters of most intense Raman mode ($E_{g(1)}$) for fresh catalysts.

Catalyst	Wavenumber (cm^{-1})	FWHM (cm^{-1})	Intensity (a.u.)
2% Ir /TiO_2	147	13.1	34.8
2% Au /TiO_2	150	20.1	25.1
2% Au-2%Ir /TiO_2	152	23.4	21.9

4. Discussion

Comments on the synergy at low temperature of Au-Ir/TiO_2 catalysts for toluene total oxidation

A strong synergetic effect in the total oxidation of toluene has been observed in Au-Ir/TiO_2 catalyst compared to their monometallic counterparts. This effect does not seem to be related to modifications in the oxidation state as no appreciable different trends have been detected by XPS. On the other hand, according to the microscopy, Au-Ir alloy has not been formed and therefore alloying phenomenon neither explains the enhanced performance of the bimetallic catalyst.

Oxidation reactions on metal supported catalysts is believed to follow the Mars van Krevelen mechanism where the adsorbed reactant is oxidised by O_{ad} atoms present on the surface

support or metal-support interface creating an oxygen vacancy. The redox cycle is then completed by oxidation of these vacancy sites by O_2 from the gas phase. However, this reaction mechanism is more complex on gold-based catalysts than in Pt or Pd ones [29], as gold plays a key role on promoting the adsorption of VOCs. As mentioned before, the bimetallic Au-Ir/TiO_2 catalyst shows an enhancement of toluene oxidation activity versus the monometallic gold and iridium catalysts, showing activity at a considerably lower temperature. In the total oxidation of toluene, the rate of reaction seems to be dictated by the dissociation of O_2 to yield atomic oxygen on the oxygen vacancies near the metal–support interface. Since in the bimetallic catalysts oxygen defects are more relevant, gold activity is promoted by the presence of Ir by facilitating the oxygen mobility at the gold-support interlayer. Thus, there is a synergetic effect in the toluene total oxidation over Au-Ir/TiO_2 catalyst, which can be associated to a stronger metal-support interaction (as evidenced by TPR), promoting the presence of a higher number of oxygen defects at the metal-support interface (as evidenced by Raman spectroscopy) and leading to an overall enhancement of activity. These observations are in agreement with previous considerations, supporting that the increase in the adhesion energy of the bimetallic slabs to the TiO_2 support caused by the presence of iridium [13], leads to a strong metal-support interaction.

Comments on the stability of Au-Ir/TiO_2 catalysts

All mono- and bi-metallic catalysts are stable if working under mild conditions (up to 300°C) for up to 3 cycles. However, if they are used at 400ºC for 20 h the catalyst activities decay. The degree of deactivation is much lower in the bimetallic catalyst than in only Au-catalyst. Therefore the presence of iridium diminishes the deactivation. XPS analyses of both Au/TiO_2 and Au-Ir/TiO_2 catalysts post-reaction (Table 2) reveals the full reduction of the gold species in both types of stability experiments. On the other hand, a marginal increase of Ir^{4+} species is observed during the two types of stability tests, decreasing the Ir^0 concentration from 20% in

the fresh catalyst to 14-18%. This small change was also observed in the Ir/TiO_2 monometallic catalysts (not shown for clarity). Therefore, the modification of the metal oxidation states does not seem to be the reason behind the different deactivation degree for both catalysts.

Agglomeration or particle growth under high temperatures is a frequent cause associated to loss of activity during high temperature reaction [15]. A similar increase in particle size from *ca.* 2 nm to ca. 5 nm was observed after 3 cycles in both, the bimetallic and monometallic gold-based catalysts and this did not originate a loss in the catalytic activity. However, after use at 400ºC, a different sintering degree was observed. Thus, in monometallic Au/TiO_2 catalyst a severe agglomeration of gold crystallites took place leading to a mean value of 13 nm. Differently in the bimetallic catalyst the domains increased but to a lesser extent, until *ca.* 7 nm.

Additionally, localized EDS analysis in nanoproble mode was used. A representative EDS spectrum ($AuIr/TiO_2$ after reaction at 400ºC) of a small area containing gold and iridium nanoparticles on titania matrix. Ti, O, Au and Ir atoms are only detected in the spectrum. The average composition of different large areas of sample was found to be in the order of 87.6, 11.4 and 1 at. % of Ti, Au and Ir respectively. The measured amount of Au, depending of the analysed area, varied between 2 and 16 at %. The higher concentration of gold was justified and related to the presence of some agglomeration of gold nanoparticles. In order to study the composition distribution of Au and Ir in bimetallic $Au\text{-}Ir/TiO_2$ used sample, EDS mapping in nanoprobe mode was conducted using a spot size in the order of 1-2 nm in diameter. As we can observe on EDS-mapping images (Figure 9), the Ir distribution on titania matrix was homogenous but the Au content distribution presents some irregularities. Results show that both elements, Au and Ir, are located in the same small nanoparticles detected on the TiO_2 support, whilst some areas are covered by either Au or Ir. The presence of agglomerated gold

nanoparticles is predominant at those zones with lower concentration of Ir. These results suggest that the presence of Ir considerably reduces the mobility of Au due to their intimate contact while promoting an enhanced gold-support interaction in the presence of Ir. These observations are in agreement with reported simulation results, in which high dispersion of a more active oxide (IrO_2) on an inert oxide (TiO_2) was predicted to preserve the sintering resistance of Au when supported on hardly active oxides [13]. These results are also in accordance with the fact that bimetallic Au-Ir catalyst promotes oxidative reactions that occur on the Au/active oxide interface [12]. According to these results, it seems that the oxidation of toluene on the monometallic Au/TiO_2 and bimetallic $Au\text{-}Ir/TiO_2$ catalysts is not very sensitive to an increase in the metal particle under the experimental condition used in this work whenever the particles are ranging from 2 to 6 nm. However, if the metal particles are larger, as those of the catalysts heat-treated at 400ºC, a remarkable decrease in the catalytic activity was observed. This decrease in activity is more notorious in the case of the Au catalyst than in the Au-Ir catalyst and this is related to the different degree of sintering (5-20 nm for Au catalyst or 3-10 nm for AuIr catalyst).

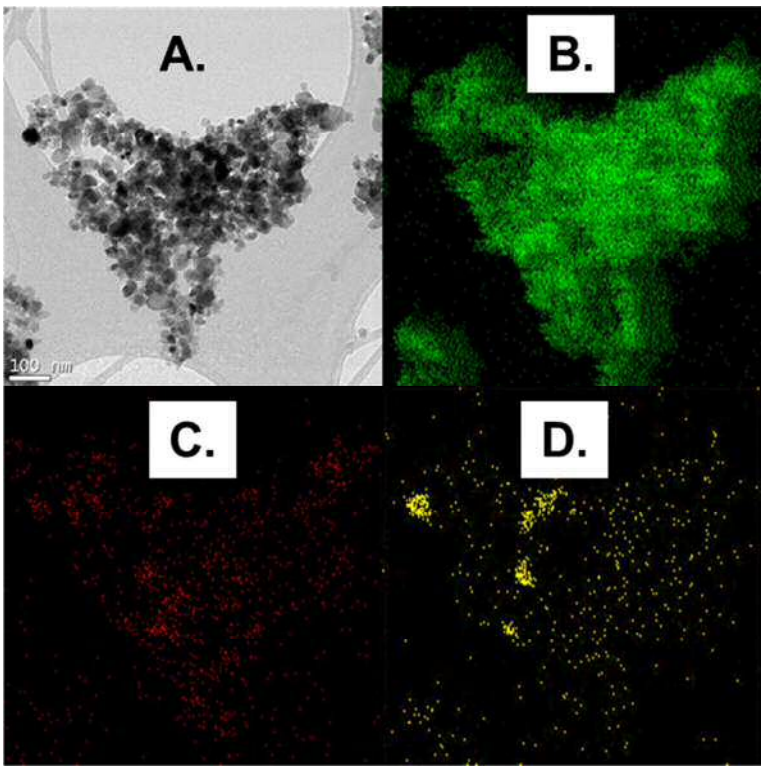

Figure 9: A. TEM image of the Au-Ir/TiO_2 catalyst after reaction at 400°C B. Ti C. Ir and D. Au maps superimposed on the experimental TEM image.

5. Conclusions

Bimetallic Au-Ir/TiO_2 catalysts shows activity for the total oxidation of toluene at considerably lower temperatures than the corresponding monometallic Au/TiO_2 or Ir/TiO_2 catalysts. This synergetic effect between gold and iridium is related to a strong metal-support interaction, which consequently increased the number of support oxygen defects at the metal-support interface, capable of activating O_2 at lower temperatures. In addition, this stronger metal-support interaction not only contributes to the low temperature activity but also to the resistance of the bimetallic Au-Ir/TiO_2 catalysts against sintering under high temperature reaction conditions.

Acknowledgements

The authors would like to acknowledge the UK Engineering and Physical Science Research Council (EPSRC, grant number EP/L020432/2), PAPIIT-UNAM (IN105416 grant) and CONACYT-APN (1216 grant) for funding.

References

[1] M.R. Heck, R.J. Farrauto, Catalytic Pollution Control, New York, 2002.
[2] S. Scire, L.F. Liotta, Appl. Catal. B-Environ. 125 (2012) 222-246.
[3] I.P.o.C.C.I.r.o. VOCs, https://www.ipcc.ch/ipccreports/tar/wg1/140.htm, 2009.
[4] L. Torrente-Murciano, A. Gilbank, B. Puertolas, T. Garcia, B. Solsona, D. Chadwick, Applied Catalysis B: Environmental 132–133 (2013) 116-122.
[5] J.M. López, A.L. Gilbank, T. García, B. Solsona, S. Agouram, L. Torrente-Murciano, Applied Catalysis B: Environmental 174–175 (2015) 403-412.
[6] T. Garcia, B. Solsona, S.H. Taylor, Catalysis Letters 105 (2005) 183-189.
[7] M. Haruta, Catal. Today 36 (1997) 153-166.
[8] L. Guczi, G. Peto, A. Beck, K. Frey, O. Geszti, G. Molnar, C. Daroczi, J. Am. Chem. Soc. 125 (2003) 4332-4337.
[9] M.M. Schubert, S. Hackenberg, A.C. van Veen, M. Muhler, V. Plzak, R.J. Behm, J. Catal. 197 (2001) 113-122.
[10] F.C. Walsh, D.V. Bavykin, L. Torrente-Murciano, A.A. Lapkin, B.A. Cressey, Trans. Inst. Metal Finish. 84 (2006) 293-299.
[11] L. Torrente-Murciano, T. Villager, D. Chadwick, ChemCatChem 7 (2015) 925-927.
[12] Z.P. Liu, S.J. Jenkins, D.A. King, Phys. Rev. Lett. 93 (2004) 4.
[13] C.W. Han, P. Majumdar, E.E. Marinero, A. Aguilar-Tapia, R. Zanella, J. Greeley, V. Ortalan, Nano Lett. 15 (2015) 8141-8147.
[14] M. Sankar, N. Dimitratos, P.J. Miedziak, P.P. Wells, C.J. Kiely, G.J. Hutchings, Chem. Soc. Rev. 41 (2012) 8099-8139.
[15] L. Torrente-Murciano, Q. He, G.J. Hutchings, C.J. Kiely, D. Chadwick, ChemCatChem 6 (2014) 2531–2534.
[16] A. Gomez-Cortes, G. Diaz, R. Zanella, H. Ramirez, P. Santiago, J.M. Saniger, J. Phys. Chem. C 113 (2009) 9710-9720.
[17] R. Zanella, S. Giorgio, C.R. Henry, C. Louis, J. Phys. Chem. B 106 (2002) 7634-7642.
[18] T.V. Choudhary, S. Banerjee, V.R. Choudhary, Appl. Catal. A-Gen. 234 (2002) 1-23.
[19] S. Krishnamurthy, G.R. Landolt, H.J. Schoennagel, J. Catal. 78 (1982) 319-326.
[20] L. Torrente-Murciano, J. Nanopart. Res. 18 (2016) 7.
[21] A. Aguirre, C.E. Barrios, A. Aguilar-Tapia, R. Zanella, M.A. Baltanas, S.E. Collins, Top. Catal. 59 (2016) 347-356.
[22] H. Hasen, Constitution of Binary Alloys, McGraw-Hill, New York, 1958.
[23] A.K. Hill, L. Torrente-Murciano, Applied Catalysis B: Environmental 172–173 (2015) 129-135.
[24] M.P. Casaletto, A. Longo, A. Martorana, A. Prestianni, A.M. Venezia, Surf. Interface Anal. 38 (2006) 215-218.
[25] J. Zhao, J. Ni, J.H. Xu, J.T. Xu, J. Cen, X.N. Li, Catal. Commun. 54 (2014) 72-76.
[26] M. Hinojosa-Reyes, R. Zanella, V. Maturano-Rojas, V. Rodriguez-Gonzalez, Appl. Surf. Sci. 368 (2016) 224-232.
[27] T. Ohsaka, F. Izumi, Y. Fujiki, J. Raman Spectrosc. 7 (1978) 321-324.
[28] N. Lopez, J.K. Norskov, Surf. Sci. 515 (2002) 175-186.

[29] G.C. Bond, D.T. Thompson, Gold Bull. 33 (2000) 41-51.